Evaluating Tools for Collective Soil Excavation: Challenges and Insights

Sean Even[1], Omer Kurkutlu[1], and Yasemin Ozkan-Aydin[1]

University of Notre Dame, Notre Dame, IN, 46556,
yozkanay@nd.edu, https://www.minirolab.nd.edu

Abstract. Achieving effective collective excavation with terrestrial robot swarms in unknown, cluttered environments presents significant challenges. These limitations primarily stem from: (1) the absence of robust, scalable collective control algorithms relying solely on local information and communication; (2) the inherent mobility constraints of terrestrial robots operating in complex terrains; and (3) a critical shortage of modular tools suitable for efficient excavation across diverse environments. In this study, we addressed the crucial preliminary step toward developing functional robotic excavation systems: effective tool characterization. We designed and implemented an automated testing apparatus to systematically evaluate various digging tools and identify key operational challenges under conditions closely mimicking real-world settings. This comprehensive assessment informed the subsequent design and optimization of excavation mechanisms and strategies for a swarm of autonomous robots, allowing for the refinement of their environmental interactions and the finalization of critical robotic components essential for effective collective excavation.

Keywords: swarm robotics, collective excavation, excavation tools, soil mechanics

Introduction

Collective excavation holds promise for everything from subterranean mapping to planetary habitat construction (see Figure 1). In nature, ants and other burrowing species [1,2] coordinate effectively to dig extensive tunnel networks in challenging soil conditions. In engineering contexts, however, multi-robot solutions must grapple with partial observability, unpredictable soils, and limited communication [3,4]. Traditional single large drills or tunnel-boring machines [**?**,5] can be powerful but lack redundancy and fine-grained adaptability. By contrast, deploying many smaller agents—if each is equipped with reliable excavation mechanisms—enables resilience in uncertain terrain. Smaller, mobile robots can access confined or difficult-to-reach areas that large excavators cannot, and different robots can specialize in specific tasks, with some for bulk material removal, others for soil preparation or precise hole drilling. A swarm also allows for the distribution of tasks across multiple units. This significantly speeds up large-scale projects compared to a single, large excavator.

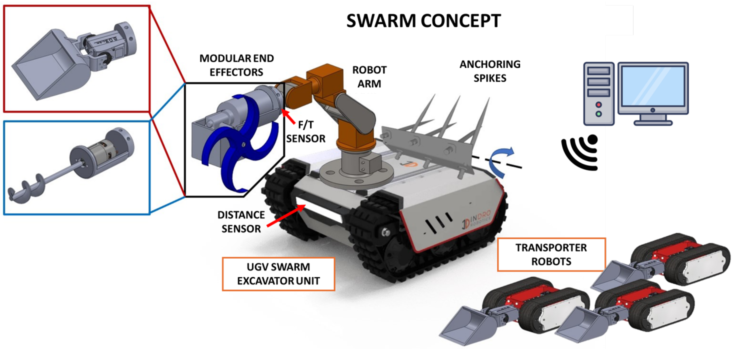

Fig. 1: **Swarm excavation concept.** Conceptual illustration of a multi-robot swarm configured for coordinated soil excavation. Each robot is equipped with a digging tool and local sensing.

Yet, before scaling to a swarm, it is essential to identify appropriate end effectors and measure how soil states (moisture, compaction) affect excavation. Notably, no single tool exists that can reliably burrow through all real-world soil conditions. We thus built an automated testbed to systematically evaluate multiple digging tools under varying soil conditions. This approach ensures that when we eventually field a multi-robot system, we deploy end effectors optimized for volume flow rate, reliability, and minimal clogging in typical soils.

Technical Approach

Excavation tasks range from loading a pile of soil to cutting a geometrically described volume of earth. In both biological and engineered systems, the properties of the soil are one of the most important factors that affect the performance of the excavation as well as tunnel stability and structure [6,2]. Since the soil is deformable, a complete state-space description of the terrain to be excavated requires a high-dimensional representation. But, for the state-based representations that traditional planners use, very large spaces are simply infeasible. Furthermore, the response of soil varies immensely, and in general, it is not possible to analytically describe the mechanics of soil motion and its interaction with robots [7,8]. A soil's shear strength depends not only on its physical and chemical properties but also on factors such as the compaction experienced in the past. Thus, a robotic excavator is forced to deal with approximate and incomplete models of its actions and their results.

Soil Conditions. We designed parametric experiments to span the range of different levels of soil compactness and cohesiveness. The compactness of the soil was modified by applying known pressure to the soil surface, and the cohesiveness was modified by varying the humidity level of the soil. Ultimately, these laboratory soil tests helped us to understand and address the effects of various soil parameters on the excavation process and provided data on which excavation mechanisms and strategies are the best for excavation for a given type of soil. These tests also helped us to determine how to position the excavation mechanism onto the robots (i.e., help us to formulate the key specifications and

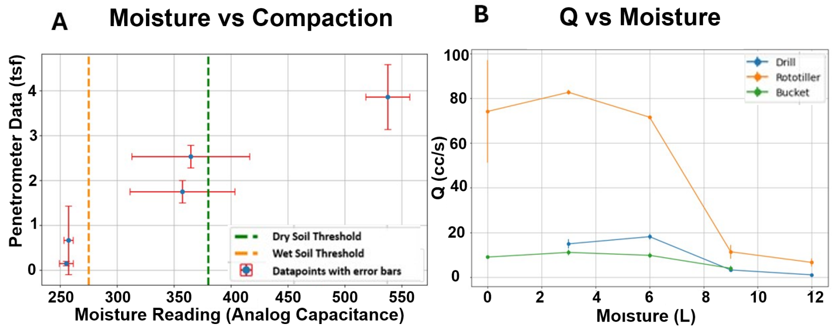

Fig. 2: **Soil Characterization.** (A) Measured soil compaction plotted against moisture content, demonstrating increased compaction with higher water levels. (B) Volume flow rate Q was recorded for three tested end effectors (horizontal axis) across varying soil moisture levels. Error bars reflect one standard deviation from three experimental trials.

features of the final design of the robots) and calculate the torque limits of the motors of the robots that will be used in the final design.

In experiments, we used silty clay (particle size < 0.05 mm, and the sand amount is less than 20%), which is cohesive soil with an unconfined compressive strength larger than 1.5 (tons/sq ft). We gradually added water in 3-liter increments to approximately 75 liters of soil, allowing each addition to permeate for about 30 minutes before the next. This process was carried out for total water additions of 0, 3, 6, 9, and 12 liters. We observed that soil compaction was directly correlated with moisture content; as moisture levels increased, so did the degree of compaction [6,2]. A standardized measurement protocol was established to determine the volume flow rate Q (cc/s), which involved measuring the volume of soil displaced along a standard 20 cm path. The relationship between moisture content and compaction is illustrated in Figure 2.

Gantry Setup. The development of fully autonomous excavation systems requires dealing with the interaction between the machine and soil [9,10]. To safely excavate a tunnel in a real environment, we need to understand the dynamics arising from the robot-earth interaction by systematically measuring the penetration forces exerted by the robots [8]. To do this, we constructed a simplified version of the tunnel environment in our laboratory. We transformed an Openbuilds CNC 1010 machine into a versatile digging apparatus, as depicted in Figure 3, SI Movie, 00:31-00:40 s). All axes of the gantry are actuated via stepper motors controlled by an Arduino MEGA 2560 microcontroller and four DM542T stepper drivers. Stepper motors were chosen for their precision and ability to provide controlled motion in incremental steps, which is important for accurate positioning during excavation.

Maintaining the original X/Y gantry configuration, we introduced several key modifications to enhance its functionality. Firstly, we mounted a compact robotic arm onto the gantry's carriage z-axis. This arm operates within a vertical plane, providing three degrees of freedom (3 DoF), and is equipped with the Robotiq

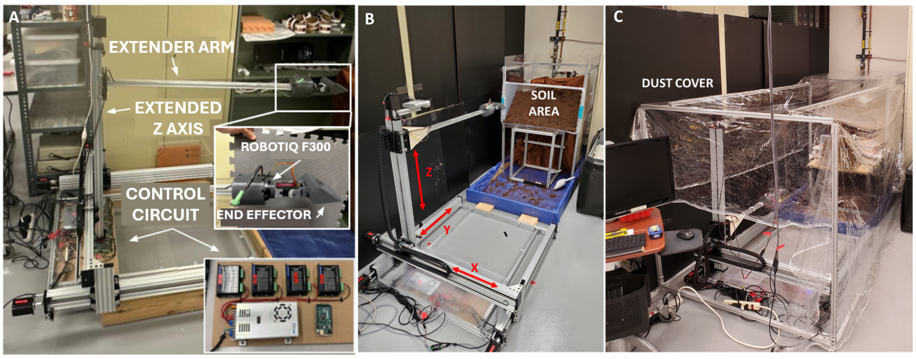

Fig. 3: **Modified CNC-based digging testbed.** The setup includes a three-degree-of-freedom (3-DoF) arm and a swappable end effector port. The rototiller end effector operating in tamped soil is shown here. A 20-cm scale bar is overlaid for size reference.

Force Torque Sensor FT300 to measure torques and forces experienced at the end effector. Secondly, we incorporated a 3D printed, modular end effector port, allowing for the swift interchange of various digging tools, such as claw scoops, augers, and rototillers. This standardized mechanical interface, featuring electrical pass-throughs, facilitates the integration of various end effectors. Lastly, we positioned a 1 m $\times$ 1 m soil-filled test box beneath the gantry. This enclosure includes a side window, enabling the observation of soil layering and compaction changes during experimentation.

End Effector	**Motor Torque**	**Weight (g)**	**Intended Use**
Rototiller	4.0 Nm	1612.06	Loosening/Removing Soil
Bucket	7.85 Nm	346.15	Removing Soil
Drill	0.43 Nm	798.69	Loosening Soil

Table 1: Specifications and intended use of various end effectors.

End Effectors Under Test. For our robotic swarm concept, we evaluated three end effector types: the bucket, auger drill, and rototiller (Figure 3). We prioritized their real-world applicability to scenarios such as excavating and transporting bulk material (bucket), drilling precise foundation or anchor holes (auger drill), and preparing or loosening compacted soil before excavation (rototiller). Each tool was assessed specifically for its practical effectiveness and suitability within collaborative excavation operations, simulating realistic conditions a robotic swarm would encounter in field deployments. Each was run under identical toolpath scripts at multiple speeds. We tracked the depth, side force, and reaction torque measured in the end effector.

Experiments

We conducted a total of 72 controlled runs, each repeating the same linear pass with a given end effector, moisture, and compaction setting. For each excavator mechanism, we separated the operation space into admissible and inadmissible

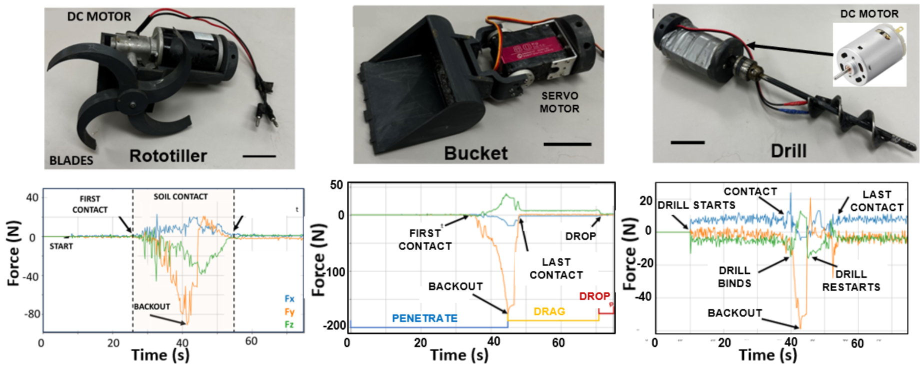

Fig. 4: **Comparison of the end effectors.** (Top row:) Final designs for the three different end effector types (rototiller, bucket, and drill). (Bottom row) Representative sensor data for each end effector, highlighting key moments in the operational cycle—such as initial motor movement and first contact with the soil. A 5 cm scale bar is included in each prototype image.

regions based on constraints posed by the mechanism and the environment. We parameterized the excavation cycle by two parameters: the approach angle of the mechanisms (an angle between the tip of the excavator mechanism and the center of mass (CoM) of the robots) and digging distance (a distance between the robot's CoM and the first contact point of soil). The volume in the operation space was excavated with different mechanisms, and we compared the mechanisms and the excavation strategies using cost functions like minimum time, minimum energy, or maximum payload.

We incorporated a Microsoft Azure Kinect depth camera to map soil surfaces, enabling targeted excavation by identifying prominent surface protrusions for digging. Initially, we trained a Detectron2 semantic segmentation network on 100 images of simulated soil, achieving reliable results even under occlusions. However, extending this approach to 3D segmentation was challenging due to noise and resolution discrepancies between depth data and 2D images, complicating keypoint matching and point cloud registration [11]. Additionally, dust interference further degraded depth sensor accuracy, making real-time surface mapping more difficult. Given these complexities, we proceeded using predefined trajectories, highlighting the necessity for future research into robust, real-time 3D mapping methods.

During each experimental run, we collected several key data sets. Firstly, time and pose data were obtained from the CNC G-code logs, allowing us to verify the tool tip's position over time. Secondly, motor load and torque measurements were recorded using sensors attached to the end effector motor's shaft. Thirdly, the excavated volume was determined by collecting and weighing the ejected soil, which was then converted to volume based on the known soil density. Utilizing these measurements, we computed the volume flow rate (Q) and analyzed its correlation with varying moisture levels and compaction degrees to identify the optimal end effector performance [9,10].

Drill End Effector The first end effector that we tested was a drill end effector (SI Movie, 01:00-01:30 s). This was inspired by augers and drills used to excavate tunnels for subways and roadways. Auger is a well-known digging mechanism that usually includes a rotating helical blade and a bit with cutters, which act as a screw conveyor to remove the drilled material [**?**].

The auger drill bit can move both in the horizontal and vertical planes. Depending on the size, shape, angular velocity, and feed rate of an auger driller, a frictional driving force exerted on the soil changes [12], which affects the performance of the extraction process. By changing the shape and size of the auger mechanism, we could calculate the optimum angular velocity and rotation speed of the different auger mechanism that works best (i.e., use less energy) for silty-clay soil.

This design is typically employed for disaggregating consolidated media, such as rock formations. The end effector's configuration is relatively straightforward, comprising a 12 V DC motor with a torque output of 0.43 Nm. This motor is coupled to a 1.6 x 9-inch hexagonal drill bit via a B10 drill chuck. The motor assembly is encapsulated within a 3D-printed housing that interfaces with a custom-fabricated universal force sensor.

Bucket End Effector The second digging mechanism is a basic, two-degree-of-freedom (2DoF) bucket-like excavator, with its height and head angle controlled by motors (SI Movie, 01:31-02:00 s). This bucket end effector is designed for handling heavier materials, incorporating capabilities such as tilt, load-and-carry, lift, and dump for efficient movement of large material volumes.

Following established excavator control literature [13], the operation of this bucket system is divided into three distinct phases: penetration, drag, and scoop. In the penetration phase, the bucket enters the soil to an effective digging depth and cutting angle. This is followed by the dragging phase, where the bucket moves parallel to the surface, causing soil to mechanically fail and accumulate. Here, the robot's forward/backward motion controls the drag forces. The final scooping phase collects the accumulated soil for transfer. To mitigate potential weight distribution issues on the robot, we kept the bucket mechanism simple, using only two motors for height and angle control.

A primary limitation of this design is its reliance on relatively loose soil for effective operation. To address this, we selected a high-torque motor providing 10.3 N.m of torque to overcome soil weight and cohesiveness. This motor is connected to a 3D-printed bucket with an internal volume of 865.5 $cm^{\mathbf{3}}$. We also designed a 3D-printed interface for the torque sensor and used an aluminum U-bracket to connect the motor assembly to our universal force sensor interface.

During operation, the bucket end effector demonstrates high effectiveness in loose soil. However, its performance significantly declines with higher soil moisture levels or if the soil has not been pre-softened by other tools, like the drill end effector. In such cases, dirt often sticks inside the bucket, reducing subsequent passes. Future iterations of this design may incorporate a prong to aid in dirt ejection during the drop phase.

Rototiller End Effector During the testing of the first two end effectors, we noticed some unique mode of failures. For the drill end effector there were two noticeable issues. The first was the tendency of the drill to bind at after the bit penetrated into the soil. Second and perhaps more consequential was the fact that the drill had a tendency to spew most of its volume sideways when its first contacted the soil. As the drill reached the point at which it would start to pull soil back it would bind. We encountered a different issue with the bucket insofar as it did not have the capability to penetrate the soil. Thus, the bucket end effector relied on a preliminary pass of an end effector that would soften the soil before it could become effective.

We addressed these issues by first integrating a 4 Nm motor, enhanced with a torque-boosting gear, housed in a 3D-printed casing. To this, we attached a newly designed excavation blade that measures 20 cm in diameter and 1 cm in thickness, featuring four circular prongs symmetrically spaced at 90 degrees. The digging implement features a notch for driving it, which is held in place by a small plate that is screwed into position (SI Movie, 02:01-02:13 s). This assembly interfaces with the force sensor using our universal force sensor interface, ensuring accurate force measurement during operation.

Force Data Analysis Analyzing force sensor data is important for evaluating end-effector efficiency in mobile robots. It provides critical insights into mechanical demands and helps identify optimal force profiles for efficient soil penetration and removal. This data not only guides improved end effector designs to withstand real-world excavation challenges but also informs the development of adaptive control algorithms that enhance robot performance and adaptability in dynamic environments through real-time feedback.

Force sensor data were consistently logged for analysis during each soil test. Figure 4 presents a comparison of forces experienced across different end effectors during a 3L trial. The bucket end effector demonstrated very low noise levels and a distinct cyclical pattern in its soil interactions, reflecting its consistent penetration, drag, and drop phases. Notably, it experienced forces orders of magnitude higher than other end effectors due to its passive nature and larger soil contact area. Conversely, the drill end effector proved to be the noisiest, with its high rotational speed introducing significant vibrations and irregularities in the force data. Force spikes were observed when the drill bound in the soil, indicating moments of high resistance. Despite these spikes, the drill experienced the lowest overall forces due to its smaller profile, which limited surface interaction. The rototiller end effector exhibited noise levels between the drill and bucket. It also showed force spikes in the y-direction during binding events, though its noise was less pronounced than the drill's due to a slower rotational speed, yet still more significant than the bucket's.

The force data helped identify the most suitable end effector design for specific soil conditions and guides improvements in excavation strategies. The bucket end effector, which experienced the highest forces, is most effective for scooping up loose soil due to its large contact area and ability to handle high resistance. In contrast, the drill end effector generated significant vibrations and frequently

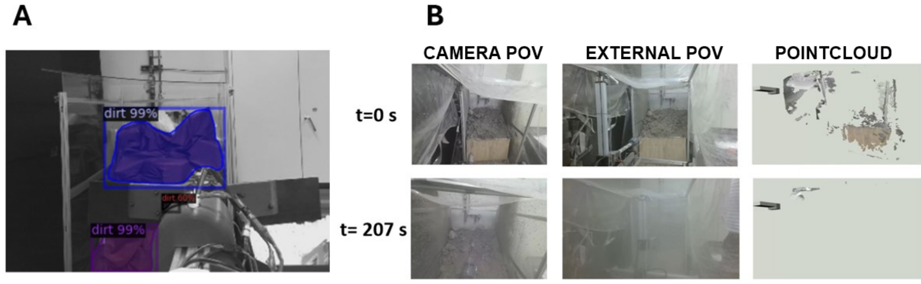

Fig. 5: **Image analysis.** (A) Example of 2D semantic segmentation of soil in the testbed, generated by a Detectron2-based network. (B) Photograph of the depth camera's view under low moisture conditions, highlighting dust that obscures the digging surface. A 10-cm scale bar is included to indicate the camera's approximate field of view.

became bound in the soil, indicating its limited suitability for continuous operation in varying soil conditions, especially on cohesive media. The rototiller end effector operated smoothly with less noise and minimal binding, demonstrating its efficiency; however, its substantial weight of approximately 2 kilograms necessitates the use of powerful motors for mobile robot integration. These findings underscore the importance of selecting appropriate end effectors based on specific excavation requirements and the mechanical capabilities of the robotic system.

Regarding moisture content, all end effectors experienced reduced efficiency when soil moisture exceeded 6 liters. However, the rototiller exhibited greater resilience under these conditions, despite occasional torque spikes in highly compacted or damp areas.

Vision and Surface Mapping A core objective was to integrate a depth camera for real-time soil surface mapping and dynamic excavation decision-making, particularly identifying optimal digging locations. This necessitated point cloud segmentation, initially approached through 2D image segmentation to differentiate soil from irrelevant areas in the field of view.

Given the significant variance in image characteristics, a Neural Network (NN) approach was selected for segmentation due to its robustness to scale, distortion, and lighting [14,15]. Since the end effector frequently obscured the soil surface, semantic segmentation was employed to classify each pixel as "dirt" [16,17]. We leveraged Detectron2, a highly effective semantic segmentation network [18], which performs well even with small datasets. To validate this, we trained Detectron2 on 100 images of brown cloth simulating soil. The network remarkably identified "soil" locations in test setups, proving robust to camera placement and end effector occlusion, despite the limited training data.

Extending this to 3D segmentation using point cloud images (3D data points with color and depth) proved challenging. Initial point cloud data, fusing depth sensor and camera information, exhibited significant noise, even in stable environments. Relying solely on depth sensor data reduced noise, but subsequent soil tests introduced new issues. Dust from excavation increased noise, and camera accuracy dropped significantly at lower soil moisture levels (SI Movie, 02:14 s). Moreover, the constantly changing soil surface demanded highly efficient processing for dynamic trajectory generation. Given these complexities, dynamic trajectories were deferred, and a predefined trajectory was used for end effector testing. We recognize that a robust vision system capable of handling these environmental complexities is critical for a fully autonomous system, constituting a significant and independent research area for future work.

Conclusions and Future Work

Soil Variability is Critical. Even minor fluctuations in moisture content or compaction levels resulted in significant changes in the volume flow rate (Q). This finding suggests that, in practical applications, implementing local sensing and dynamic adjustments to tool parameters, such as speed or angle, may be essential to maintain optimal performance [19,2].
Robust End Effector Mechanisms. The superior performance of the rototiller can be attributed to its multi-tooth engagement design, which facilitates more uniform soil disruption. In contrast, tools like bucket wheels are prone to jamming unless they are appropriately sized and powered, highlighting the importance of robust mechanical design in end effectors [5].
Automated setup. Utilizing a CNC-based test rig enabled repeatable experiments and rapid iteration of design modifications. Such testbeds are invaluable in the early stages of development, particularly when scaling solutions to swarm robotics applications. They allow for the identification of hardware constraints before deploying distributed and autonomous systems, thereby enhancing the reliability and effectiveness of the final implementation [3].
Challenges to be Addressed in a Multi-Robot System Deploying multi-robot excavation systems presents key challenges, including collision risks from simultaneous digging, disrupted communication in subterranean environments, and coordination issues due to unorganized soil removal. Additionally, handling soil variability and jams in dense or rocky patches requires adaptive tools, such as adjustable feed rates or vibrational techniques. Successful field deployment will likely depend on robust local sensing of moisture and compaction to dynamically adjust excavation strategies, potentially integrating specialized tools and retractable guards to minimize interference among robots. Our systematic evaluation using a CNC-based testbed identified the rototiller as the most effective end effector, offering robustness across varied soil conditions and minimal jamming incidents. Future multi-robot systems could significantly benefit from combining this design with localized sensing and dynamic adaptation, enabling swarms to operate efficiently in unpredictable subterranean environments, fulfilling the potential for collective tunnel-building.

References

1. Monaenkova, D. *et al.* Behavioral and mechanical determinants of collective subsurface nest excavation. *J Exp Biol* **218**, 1295–305, (2015).

2. Macedo, R. *et al.* Unearthing real-time 3d ant tunneling mechanics. *Proceedings of the National Academy of Sciences* **118**, 2102267118, (2021).
3. Werfel, J., Petersen, K. & Nagpal, R. Designing collective behavior in a termite-inspired robot construction team. *Science* **343**, 754–758 (2014).
4. Aina, K. *et al.* Toward task capable active matter: Learning to avoid clogging in confined collectives via collisions. *Frontiers in Physics* **10** (2022).
5. Bar-Cohen, Y. & Zacny, K. *Drilling in Extreme Environments: Penetration and Sampling on Earth and other Planets* (Wiley, 2009).
6. Frost, J. *et al.* Biologically-inspired insight into soil arching and tunnel stability from the topology of ant nests. In *19th International Conference on Soil Mechanics and Geotechnical Engineering* (2017).
7. Nguyen, D.-H., Azéma, E., Sornay, P. & Radjai, F. Effects of shape and size polydispersity on strength properties of granular materials. *Phys. Rev. E* **91**, 032203, (2015).
8. Nedorezov, I. Technical note: Statistical estimates of soil cutting resistances for excavating robots. In *Automation and Robotics in Construction Xi, Elsevier*, 277–280, (1994).
9. Sotiropoulos, F. & Asada, H. A model-free extremum-seeking approach to autonomous excavator control based on output power maximization. *IEEE Robotics and Automation Letters* **4**, 1005–1012, (2019).
10. Dadhich.S, U. & Andersson, U. Key challenges in automation of earth-moving machines. *Automation in Construction* **68**, 212–222, (2016).
11. Roucek, T. Darpa subterranean challenge: Multi-robotic exploration of underground environments. In *Modelling and Simulation for Autonomous Systems*, 274–290 (Springer International Publishing, 2020).
12. Tan, S., Duan, L., Guo, Z. & Gao, H. Theoretical derivation of the cuttings transportation trajectory for lunar sampling auger drilling. *International Journal of Rock Mechanics & Mining Sciences* **86**, 204–209, (2016).
13. Sotiropoulos, F. & Asada, H. A model free extremum seeking approach to autonomous excavator control based on output power maximization. *IEEE Robotics and Automation Letters* **4**, 1005–1012, (2019).
14. Krizhevsky, A., Sutskever, I. & Hinton, G. E. Imagenet classification with deep convolutional neural networks. In Pereira, F., Burges, C., Bottou, L. & Weinberger, K. (eds.) *Advances in Neural Information Processing Systems*, vol. 25 (Curran Associates, Inc., 2012).
15. Simonyan, K. & Zisserman, A. Very deep convolutional networks for large-scale image recognition. In *International Conference on Learning Representations* (2015).
16. Long, J., Shelhamer, E. & Darrell, T. Fully convolutional networks for semantic segmentation. In *2015 IEEE Conference on Computer Vision and Pattern Recognition (CVPR)*, 3431–3440 (2015).
17. Chen, L.-C., Papandreou, G., Kokkinos, I., Murphy, K. & Yuille, A. L. Deeplab: Semantic image segmentation with deep convolutional nets, atrous convolution, and fully connected crfs. *IEEE Transactions on Pattern Analysis and Machine Intelligence* **40**, 834–848 (2018).
18. Kirillov, A., Wu, Y., He, K. & Girshick, R. Pointrend: Image segmentation as rendering (2020). 1912.08193.
19. Nguyen, E. Effects of shape and size polydispersity on strength properties of granular materials. *Phys. Rev. E Stat. Nonlin. Soft Matter Phys* **91**, 032203 (2015).